Bouncing ball on a vibrating periodic surface

Avishai Halev, and Daniel M. Harris

Citation: Chaos **28**, 096103 (2018); doi: 10.1063/1.5023397
View online: https://doi.org/10.1063/1.5023397
View Table of Contents: http://aip.scitation.org/toc/cha/28/9
Published by the American Institute of Physics

Bouncing ball on a vibrating periodic surface

Avishai Halev and Daniel M. Harris[a)]
Department of Mathematics, University of North Carolina at Chapel Hill, Chapel Hill, North Carolina 27599, USA

(Received 23 January 2018; accepted 26 March 2018; published online 13 September 2018)

We present an investigation of a partially elastic ball bouncing on a vertically vibrated sinusoidal surface. Following the work of McBennett and Harris [Chaos **26**, 093105 (2016)], we begin by demonstrating that simple periodic vertical bouncing at a local minimum of the surface becomes unstable when the local curvature exceeds a critical value. The resulting instability gives rise to a period doubling cascade and results in persistent horizontal motion of the ball. Following this transition to horizontal motion, periodic "walking" states—where the ball bounces one wavelength over each vibration cycle—are possible and manifest for a range of parameters. Furthermore, we show that net horizontal motion in a preferred direction can be induced by breaking the left-right symmetry of the periodic topography. *Published by AIP Publishing.* https://doi.org/10.1063/1.5023397

When a ball bounces on a vibrating wavy surface, one might expect the ball to ultimately become trapped within a valley and bounce in place. While this fate is possible in some cases, we show that a periodic impact surface can actually induce persistent horizontal motion of the ball along the surface. A variety of different possible motions are observed, including a "walking" state wherein the ball advances regularly in one direction along the surface. The final direction of motion of such walking states is highly sensitive to both initial conditions and the symmetry of the underlying surface.

I. INTRODUCTION

Fluid droplets may bounce indefinitely on a vibrating fluid bath, exhibiting complex vertical dynamics which depend sensitively on the droplet size, characteristics of the fluid, and the vibration profile.[2–4] At each impact with the underlying bath, the droplet deforms the free surface, generating waves at the interface. In certain parameter regimes, the droplets can interact with the waves created at previous impacts and begin to progress horizontally across the surface.[5,6] This fluid system represents a macroscopic wave-particle duality and has been shown to have behaviors reminiscent of some single-particle quantum systems.[7,8] In this work, we explore the dynamics of a simpler bouncer system and demonstrate that the interaction of a bouncer and *fixed* waveform can similarly lead to directed motion and other exotic dynamics.

This complex fluid system is reminiscent of the celebrated bouncing ball problem, wherein a ball bounces repeatedly on a vibrating rigid platform. This problem has been investigated for decades and still constitutes an active area of research. The basic physical system is conceptually simple yet exhibits surprisingly rich dynamical behaviors.[9] The one-dimensional problem, wherein the ball bounces vertically on a flat platform in a gravitational field, is the scenario most frequently explored in the literature.[10–25] Some extensions of the 1D case have focused on multiple spatial dimensions where the ball is not physically constrained in the horizontal direction and bounces on a non-flat topography.[1,26–29] In particular, it has recently been demonstrated in both experiment and theory that a concave impact surface can actually *destabilize* purely vertical bouncing and result in persistent horizontal motion of the ball.[1,29] It has been shown that directed horizontal motion of passive bouncers can be achieved by breaking the symmetry of the vibration,[30] the individual particles,[31] or the impact surface.[32] For many applications in granular or soft matter physics, achieving net horizontal motion of individual particles is desirable.

In the present work, we explore the classical two-dimensional bouncer model with an underlying periodic topography. For the case of a sinusoidal impact surface, we demonstrate that a critical curvature exists beyond which purely vertical bouncing at a minimum becomes unstable and horizontal motion naturally ensues. Ultimately, the particle can escape a single wavelength and bounce horizontally in irregular (diffusive-like) or regular bouncing modes. Additionally, we demonstrate that even a slight breaking of the lateral surface symmetry can result in a net directed motion of individual bouncers.

II. THE 2D MODEL

In this work, we investigate the motion of a partially elastic ball bouncing on a vibrating platform with sinusoidal topography. We employ the 2D model as outlined in McBennett and Harris,[1] but with a vibrating platform of surface height

$$h(x,t) = -A\cos(kx) + \gamma\sin(\omega t), \tag{1}$$

where A and k are the amplitude and wavenumber, respectively, of the static topography. From here on, we work in non-dimensional coordinates, using the time scale $\frac{2\pi}{\omega}$ and the length scale $\frac{2\pi^2 g}{\omega^2}$ as in Luck and Mehta.[14] This choice results

a)Present address: School of Engineering, Brown University, Providence, RI 02912, USA; daniel_harris3@brown.edu

in the dimensionless surface height

$$\psi(\xi,\tau) = f(\xi) + g(\tau) = -\frac{\eta}{2\pi}\cos(\chi\xi) + \frac{\Gamma}{2\pi}\sin(2\pi\tau), \quad (2)$$

where τ and ξ are the non-dimensional time and horizontal coordinates, respectively. Furthermore, we define dimensionless sinusoidal amplitude $\eta = \frac{A\omega^2}{\pi g}$, wavenumber $\chi = \frac{2\pi^2 gk}{\omega^2}$, and plate amplitude $\Gamma = \frac{\gamma\omega^2}{\pi g}$, where g is the acceleration due to gravity.

The 2D model of McBennett and Harris[1] has four independent quantities that are updated and recorded at each successive impact n: the time at which contact occurs (τ_n), the vertical and horizontal take-off velocities (v_n and u_n, respectively), and the horizontal location of impact (ξ_n). The free-flight equations along with relations for updating the relative velocities after impact define an implicit map for the system $(\tau_n, v_n, u_n, \xi_n) \to (\tau_{n+1}, v_{n+1}, u_{n+1}, \xi_{n+1})$. In this model, it is assumed that contact occurs instantaneously and that the relative normal and horizontal velocities are updated accordingly using a constant coefficient of restitution. The normal and tangential coefficients of restitutions are denoted as α_N and α_T, respectively, and take constant values between 0 and 1. Additionally, any effects due to a finite ball diameter, including rotation and air resistance, are neglected in the present model. We thus should emphasize that our model is for a point mass ($R = 0$) or for cases where $u_n \gg R\dot{\theta}_n$, where R and $\dot{\theta}_n$ are the dimensionless radius and rotation rate of the ball, respectively.

III. SIMPLE VERTICAL BOUNCING AND HORIZONTAL MOTION

For $\eta = 0$, the governing equations correspond to the flat-plane scenario for which Luck and Mehta[14] demonstrated that the system allows for a stable simple vertical bouncing state ($\tau_{n+1} = \tau_n + 1, v_{n+1} = v_n, u_{n+1} = u_n = 0, \xi_{n+1} = \xi_n$) when the forcing amplitude Γ lies within the following range:

$$\frac{1-\alpha_N}{1+\alpha_N} < \Gamma < \left[\left(\frac{1-\alpha_N}{1+\alpha_N}\right)^2 + \left(\frac{2(1+\alpha_N^2)}{\pi(1+\alpha_N)^2}\right)^2\right]^{1/2}. \quad (3)$$

McBennett and Harris[1] subsequently showed that such simple vertical motion is horizontally stable at the vertex of a parabola below a critical parabolic coefficient κ_c. Similarly, we observe that this simple vertical motion is also horizontally stable up to critical values of the coefficients about any minimum of the sinusoid. By conducting a linear stability analysis of the simple vertical bouncing (SVB) state, we arrive at a linearization matrix identical to that of McBennett and Harris[1] with κ corresponding to $\frac{\eta\chi^2}{4\pi}$ for the present topography. This coefficient is naturally the 2nd-order coefficient in the Taylor expansion of the sinusoid about any minimum $\xi_0 = 2m\pi/\chi, m \in \mathbb{Z}$:

$$f(\xi) \approx -\frac{\eta}{2\pi} + \frac{\eta\chi^2}{4\pi}(\xi - \xi_0)^2 + \cdots. \quad (4)$$

Beyond this region (specifically when $\frac{\eta\chi^2}{4\pi}$ exceeds a critical value), a flip bifurcation occurs resulting in persistent horizontal motion of the ball, as can be seen for a representative set of parameters in Fig. 1(a).

IV. WALKING SOLUTIONS

For a wide variety of parameters and initial conditions, periodic "walking" motion—wherein the ball periodically travels exactly one wavelength each vibration cycle—occurs. This type of state has been predicted for the conservative elastic bouncing ball system (without vibration).[33] We will explore this regime with $\alpha_N = 0.8$, $\alpha_T = 0.3$, and $\Gamma = 0.2$ (for which $\kappa_c = 1.0636\ldots$); however, qualitatively similar motion manifests for other parameters as well. Note that simple vertical bouncing on a flat plate is *stable* for these parameters, and thus any departure from this is directly attributable to the topography. For our selected parameters, walking is observed immediately after an irregular diffusive-like region as η is increased incrementally, as can be seen in Fig. 1(a). Note that while the particle under consideration in Fig. 1 walks in the negative χ direction, particles in the stable walking regime walk in the positive or negative direction with equal probability. The eventual direction of walking is highly sensitive to the initial conditions.

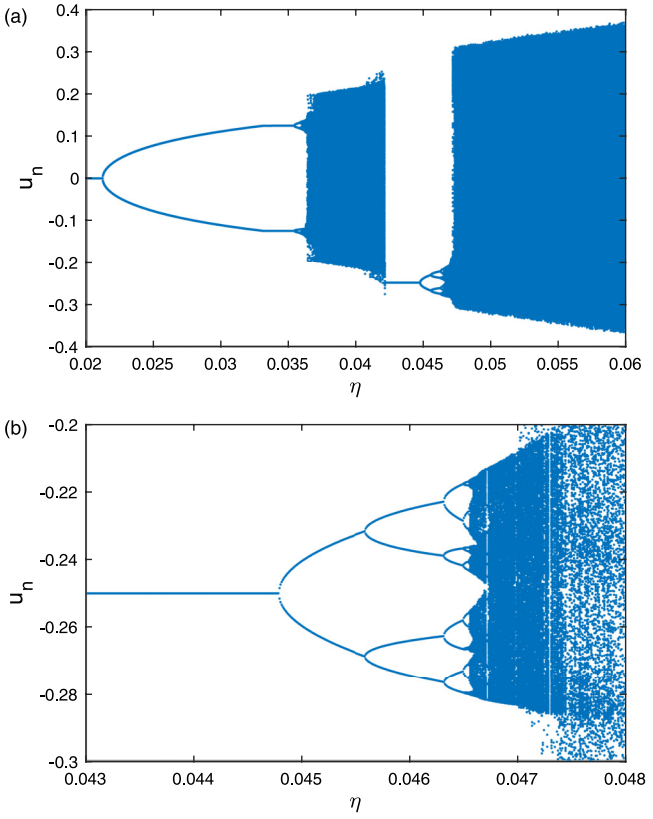

FIG. 1. (a) Numerical prediction for the last 400 horizontal velocities u_n as η is gradually increased, for the case when $\alpha_N = 0.8$, $\alpha_T = 0.3$, $\Gamma = 0.2$, and $\chi = 8\pi$. (b) Expanded view of period-doubling cascade observed following the walking region. The diagrams in the figure are for one set of initial conditions (see the supplementary material).

As the wave amplitude η is increased further, the period-one walking solutions lose their stability and a period doubling cascade is again observed, as seems to be a hallmark for the bouncing ball system. Higher modes of walking are possible and period-two, -four, -eight, and -sixteen walking states can be seen in Fig. 1(b).

While unobservable in simulation, unstable walking solutions are also possible. To further explore this walking regime, we seek all possible solutions that satisfy $\tau_{n+1} = \tau_n + 1$, $v_{n+1} = v_n$, $u_{n+1} = u_n$, and $\xi_{n+1} = \xi_n + 2\pi/\chi$. Although these conditions only find walking solutions in the positive direction, the negative walking solutions are identical through symmetry. Applying these conditions to the equations of motion,[1] the required horizontal velocity falls out immediately

$$u_* = u_n = \frac{2\pi}{\chi}. \tag{5}$$

Using the walking conditions, the vertical velocity $v_* = v_n$ can be solved for numerically as well. The resultant v_* depends only on the coefficients of restitution α_N and α_T and the wavenumber χ; it is independent of both amplitude η and forcing Γ as well as the other dynamical variables. The walking conditions also result in the necessary condition

$$v_* + \Gamma\cos(2\pi\tau_*) - 1 = 0, \tag{6}$$

where $\tau_* = \tau_n \bmod 1$. Thus, for all v_*, we have a pair of possible solutions τ_*

$$\tau_* = \pm\frac{1}{2\pi}\cos^{-1}\left(\frac{1-v_*}{\Gamma}\right). \tag{7}$$

For such solutions to exist, it must be the case that $|1 - v_*| \le \Gamma$. Since v_* is independent of η and the other dynamical variables, for any given values of α_N and α_T, there is a minimum χ for which solutions can exist as $\frac{dv_*}{d\chi} \ge 0$ and $v_* < 1$ in the relevant regime. For our chosen parameters, this critical value is $\chi_c \approx 5.21106\pi$.

Two possible positional values $\xi_* = \xi_n \bmod 2\pi/\chi$ can also be determined once v_* is known. These two points are symmetric about the sinusoid's point of inflection such that the local slope is equal at each point. The four unique combinations of τ_* and ξ_* each correspond to a possible walking solution. Again, note that corresponding solutions with $\tau = \tau_*$, $v = v_*$, $u = -u_*$, and $\xi = -\xi_*$ exist for walking in the negative direction.

For any given wavenumber $\chi \ge \chi_c$, there exists a minimum amplitude η_c such that the positional values ξ_* are real (and thus walking solutions exist):

$$\eta_c = \frac{\alpha_N + \alpha_T}{2\chi(\alpha_N + 1)}\left[(2 - v_*)\chi - \sqrt{\frac{16\pi^2(\alpha_N + 1)(\alpha_T - 1)}{(\alpha_N + \alpha_T)^2} + \chi^2(v_* - 2)^2}\right]. \tag{8}$$

While this lower bound is defined in terms of the vertical velocity, v_* itself is numerically determined from α_N, α_T, and χ; thus, this lower bound is similarly determined by only those parameters.

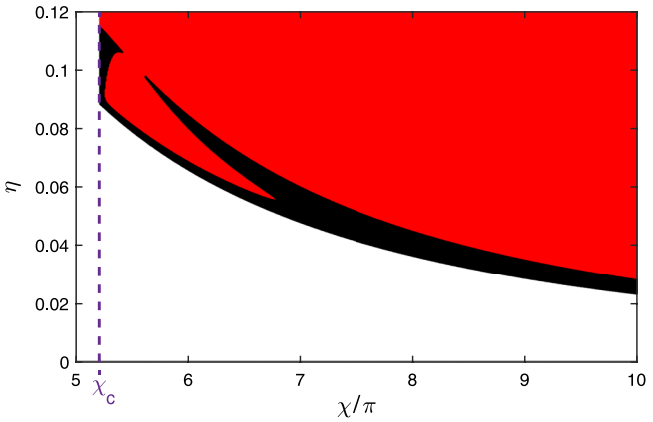

FIG. 2. Prediction for region where walking states exist (filled region) for $\alpha_N = 0.8$, $\alpha_T = 0.3$, $\Gamma = 0.2$. The black portion corresponds to points where a *stable* walking solution exists.

Of the four possible walking solutions for any given set of parameters, at most one is stable. Stability of walking solutions is determined by linearization of the governing equations about the numerically determined walking solution (see the supplementary material for extended details). By analyzing a range of values of η and χ, a map of solutions appears and the lower bounds on both parameters for walking to exist become apparent (Fig. 2). Note that while stable solutions may exist for a set of parameters, it is not guaranteed that the system will lock into those walking solutions, given the arbitrary initial conditions (or it may take a large number of bounces to do so).

V. BREAKING SYMMETRY

In many applications, directed transport of individual particles is desirable. Since motion in which the particle moves in either direction with equal probability is unhelpful in this regard, we extend our model by breaking the left-right symmetry of our sinusoidal topography in order to see if a preferred direction of motion can be induced.

To begin our discussion, consider the Fourier series for a sawtooth wave of amplitude $\frac{\eta}{2\pi}$:

$$f_s(\xi) = -\frac{\eta}{\pi^2}\sum_{n=1}^{\infty}\frac{1}{n}\sin(n\chi\xi), \tag{9}$$

which converges to a sawtooth wave for all $\xi \ne 2\pi m/\chi$, $m \in \mathbb{Z}$. Truncating this series after the second term motivates a simple functional form for continuously breaking the symmetry of the original sinusoid

$$f(\xi) = -\frac{\eta\Lambda}{2\pi}\left[\sin(\chi\xi) + \frac{\eta_2}{2}\sin(2\chi\xi)\right], \tag{10}$$

where η_2 is a selected parameter between zero and unity that measures the degree to which the symmetry is broken, and

$$\Lambda = \frac{(1 - 4\eta_2 + \mu)^2}{2(1-\eta_2)^{3/2}\sqrt{\mu - 3\eta_2}(1 - 2\eta_2 + \mu)} \tag{11}$$

fixes the peak amplitude of the topography to $\frac{\eta}{2\pi}$ for $\mu = \sqrt{1 + 8\eta_2^2}$. Sample topographies for different values of η_2 are shown in Fig. 3(a).

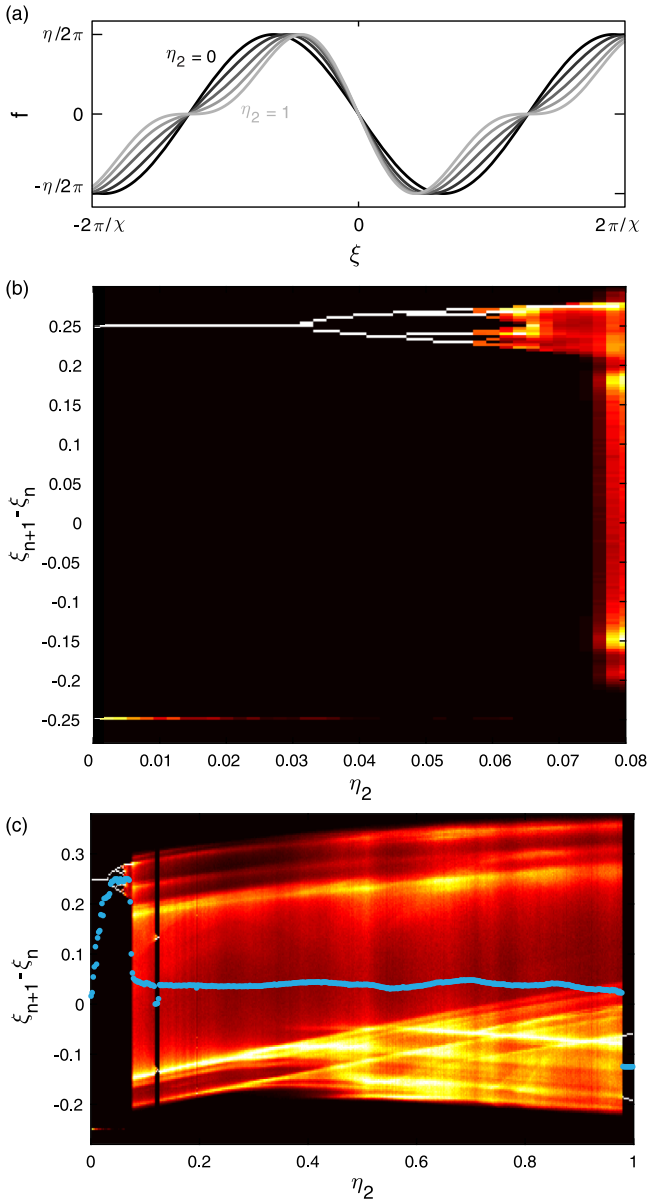

FIG. 3. (a) Example of profiles of periodic surface with increasing η_2. Curves shown are for $\eta_2 = 0, 0.25, 0.5, 0.75$, and 1 (from dark to light, respectively). [(b) and (c)] Histogram of horizontal displacements per bounce as a function of η_2. Each vertical column represents a histogram that is normalized such that the lightest (white) spot corresponds to the peak of the histogram for that given value of η_2. Each histogram is generated of the horizontal velocities observed for 100 independent balls started with different initial conditions. In part (c), the blue dots represent the time-averaged horizontal velocity.

We analyzed this system using $\eta = 0.043$ and $\chi = 8\pi$, a regime which eventually displays period-one walking with unit probability in the symmetric topography ($\eta_2 = 0$). The interval $0 < \eta_2 < 0.08$ provides the most insight into forcing walking in a preferred direction. As $\eta_2 \to 0.068\ldots$, the probability of walking in the positive direction approaches unity [Fig. 3(b)], as the likelihood of locking into a negative walking state vanishes. These increasing probabilities also align with a period doubling bifurcation of the positive walking states.

For intermediate values of η_2—approximately the range $0.1 < \eta_2 < 0.98$—the particles exhibit irregular motion but tend (on average) to drift in the positive direction. However, this motion is inefficient in that average drift rate is significantly slower than in the forced walking regime. For $\eta_2 > 0.98$, the bulk motion of the particles actually reverses the direction entirely and proceeds in the negative χ direction, locking into period-two walking such that $\xi_{n+2} - \xi_n = 2\pi/\chi$ (following an initial transient phase in the positive direction). The special case $\eta_2 = 1$ presents a unique topography; a saddle point manifests in each wavelength and simple vertical bouncing at such points becomes possible.

VI. CONCLUSIONS AND OUTLOOK

In this work, we have elucidated some of the rich behaviors possible for individual particles bouncing a vibrating impact platform with periodic topography. In particular, we identified and analyzed a new periodic "walking" state and also demonstrated that net directed motion can be achieved by breaking the horizontal symmetry of the surface topography. Enhancement of transport properties using topography could be important for applications relating to the transport or separation of vibrated granular materials[34,35] or for the manipulation of droplets on a vibrating substrate for digital microfluidics.[36]

Future work will further analyze diffusive-like behavior that manifests in various parts of the parameter space, as well as the inclusion of additional physics in order to be able to directly compare to experimental observations. In addition, we aim to consider time-dependent sinusoidal topographies which will permit us to model the motion of granular particles on a resonating plate[37–39] or of small fluid droplets bouncing on standing Faraday wave fields.

SUPPLEMENTARY MATERIAL

See supplementary material for additional details on the walking solutions and stability analysis and for movies of some possible bouncing and walking states.

ACKNOWLEDGMENTS

The authors would like to thank the Joint Applied Math and Marine Sciences Fluids Lab at the University of North Carolina at Chapel Hill for financial support and engaging discussions. D.M.H. would also like to acknowledge the financial support of the National Science Foundation (Grant No. RTG DMS-0943851).

[1]B. G. McBennett and D. M. Harris, "Horizontal stability of a bouncing ball," Chaos **26**, 093105 (2016).
[2]Y. Couder, E. Fort, C.-H. Gautier, and A. Boudaoud, "From bouncing to floating: Noncoalescence of drops on a fluid bath," Phys. Rev. Lett. **94**, 177801 (2005).
[3]J. Molácek and J. W. Bush, "Drops bouncing on a vibrating bath," J. Fluid Mech. **727**, 582–611 (2013).
[4]Ø. Wind-Willassen, J. Moláček, D. M. Harris, and J. W. Bush, "Exotic states of bouncing and walking droplets," Phys. Fluids **25**, 082002 (2013).
[5]S. Protière, A. Boudaoud, and Y. Couder, "Particle–wave association on a fluid interface," J. Fluid Mech. **554**, 85–108 (2006).
[6]J. Molácek and J. W. Bush, "Drops walking on a vibrating bath: Towards a hydrodynamic pilot-wave theory," J. Fluid Mech. **727**, 612–647 (2013).
[7]Y. Couder, S. Protiere, E. Fort, and A. Boudaoud, "Dynamical phenomena: Walking and orbiting droplets," Nature **437**, 208–208 (2005).

[8]J. W. M. Bush, "Pilot-wave hydrodynamics," Annu. Rev. Fluid Mech. **49**, 269–292 (2015).
[9]N. Tufillaro, T. Abbott, and J. Reilly, *An Experimental Approach to Nonlinear Dynamics and Chaos* (Addison-Wesley, Redwood City, CA, 1992).
[10]P. J. Holmes, "The dynamics of repeated impacts with a sinusoidally vibrating table," J. Sound Vib. **84**, 173–189 (1982).
[11]N. Tufillaro and A. Albano, "Chaotic dynamics of a bouncing ball," Am. J. Phys. **54**, 939–944 (1986).
[12]Z. J. Kowalik, M. Franaszek, and P. Pierański, "Self-reanimating chaos in the bouncing-ball system," Phys. Rev. A **37**, 4016 (1988).
[13]A. Mehta and J. Luck, "Novel temporal behavior of a nonlinear dynamical system: The completely inelastic bouncing ball," Phys. Rev. Lett. **65**, 393 (1990).
[14]J. Luck and A. Mehta, "Bouncing ball with a finite restitution: Chattering, locking, and chaos," Phys. Rev. E **48**, 3988 (1993).
[15]J. M. Hill, M. J. Jennings, D. V. To, and K. A. Williams, "Dynamics of an elastic ball bouncing on an oscillating plane and the oscillon," Appl. Math. Model. **24**, 715–732 (2000).
[16]M. Naylor, P. Sánchez, and M. R. Swift, "Chaotic dynamics of an air-damped bouncing ball," Phys. Rev. E **66**, 057201 (2002).
[17]J.-C. Géminard and C. Laroche, "Energy of a single bead bouncing on a vibrating plate: Experiments and numerical simulations," Phys. Rev. E **68**, 031305 (2003).
[18]S. Giusepponi and F. Marchesoni, "The chattering dynamics of an ideal bouncing ball," Europhys. Lett. **64**, 36 (2003).
[19]S. Giusepponi, F. Marchesoni, and M. Borromeo, "Randomness in the bouncing ball dynamics," Physica A **351**, 142–158 (2005).
[20]J. J. Barroso, M. V. Carneiro, and E. E. Macau, "Bouncing ball problem: Stability of the periodic modes," Phys. Rev. E **79**, 026206 (2009).
[21]S. Vogel and S. J. Linz, "Regular and chaotic dynamics in bouncing ball models," Int. J. Bifurcat. Chaos **21**, 869–884 (2011).
[22]A. K. Behera, A. S. Iyengar, and P. K. Panigrahi, "Non-stationary dynamics in the bouncing ball: A wavelet perspective," Chaos **24**, 043107 (2014).
[23]A. L. Livorati, I. L. Caldas, C. P. Dettmann, and E. D. Leonel, "Crises in a dissipative bouncing ball model," Phys. Lett. A **379**, 2830–2838 (2015).
[24]J.-Y. Chastaing, E. Bertin, and J.-C. Géminard, "Dynamics of a bouncing ball," Am. J. Phys. **83**, 518–524 (2015).
[25]Z. Jiang, Z. Liang, A. Wu, and R. Zheng, "Effect of collision duration on the chaotic dynamics of a ball bouncing on a vertically vibrating plate," Physica A **494**, 380–388 (2017).
[26]L. Mátyás and R. Klages, "Irregular diffusion in the bouncing ball billiard," Physica D **187**, 165–183 (2004).
[27]A. S. de Wijn and H. Kantz, "Vertical chaos and horizontal diffusion in the bouncing-ball billiard," Phys. Rev. E **75**, 046214 (2007).
[28]H. Wright, M. Swift, and P. King, "The horizontal stability of a ball bouncing upon a vertically vibrated concave surface," Europhys. Lett. **81**, 14002 (2007).
[29]J.-Y. Chastaing, G. Pillet, N. Taberlet, and J.-C. Géminard, "Transversal stability of the bouncing ball on a concave surface," Phys. Rev. E **91**, 052918 (2015).
[30]E. Sloot and N. Kruyt, "Theoretical and experimental study of the transport of granular materials by inclined vibratory conveyors," Powder Technol. **87**, 203–210 (1996).
[31]S. Dorbolo, D. Volfson, L. Tsimring, and A. Kudrolli, "Dynamics of a bouncing dimer," Phys. Rev. Lett. **95**, 044101 (2005).
[32]A. J. Bae, W. A. M. Morgado, J. Veerman, and G. L. Vasconcelos, "Single-particle model for a granular ratchet," Physica A **342**, 22–28 (2004).
[33]P. Emtage, "Motion of an elastic ball on a regularly corrugated surface," Am. J. Phys. **36**, 1126–1130 (1968).
[34]Z. Farkas, P. Tegzes, A. Vukics, and T. Vicsek, "Transitions in the horizontal transport of vertically vibrated granular layers," Phys. Rev. E **60**, 7022 (1999).
[35]X. Shi, G. Miao, and H. Zhang, "Horizontal segregation in a vertically vibrated binary granular system," Phys. Rev. E **80**, 061306 (2009).
[36]S. Daniel, M. K. Chaudhury, and P.-G. De Gennes, "Vibration-actuated drop motion on surfaces for batch microfluidic processes," Langmuir **21**, 4240–4248 (2005).
[37]T. D. Rossing, "Chladni's law for vibrating plates," Am. J. Phys. **50**, 271–274 (1982).
[38]G. Vuillermet, P.-Y. Gires, F. Casset, and C. Poulain, "Chladni patterns in a liquid at microscale," Phys. Rev. Lett. **116**, 184501 (2016).
[39]I. Grabec, "Vibration driven random walk in a Chladni experiment," Phys. Lett. A **381**, 59–64 (2017).